Optical and structural study of bismuth doped yttrium oxide

G. BHAVANI[a], S. GANESAN[b]

[a]*Department of Physics, Jansons Institute of Technology, Coimbatore, Tamilnadu, India*
[b]*Professor and Head, Sri Shakthi Institute of Engineering and Technology, Coimbatore, Tamilnadu, India*

Yttrium oxide (Y_2O_3) is an interesting host material for high power laser applications. Bi +3 is used in an attempt to activate Y_2O_3, the most promising rare-earth oxide matrix known. Bismuth doped Y_2O_3 samples are synthesized by simple precipitation techniques like sol-gel, solvothermal and wet chemical methods. Structural analysis is done by FTIR, XRD and SEM-EDAX and the optical properties are analysed by UV- Vis absorption studies and PL. UV- Vis absorption studies showed absorption only at 300 nm and PL shows two peaks around 420 nm and 440 nm. The emission peaks around 420nm and 440 nm for Y_2O_3: Bi are due to the splitting of the excited 6s6p state into $3P^0$ and $3P^1$ states, respectively, which is originated by the spin-orbital interaction.

1. Introduction

Nanomaterials with a large volume to surface area and high dielectric constant are in the focus of current interest for the further development of modern electronics. This is due to the grain barrier effects which occur at nanosize which play an important role on the dielectric properties of the materials and they exhibit novel catalytic, optical, magnetic and electrical properties relative to those of the bulk materials [1-5].The regular improvement in display market is extending its study on the next generation display devices such as organic light emitting diode (OLED) or flexible display [6, 7]. Hence a material with good optical properties has to be identified for commercial applications. One such identified host lattice is yttrium oxide.

Y_2O_3 possesses some unique properties. It has a higher melting temperature (2430°C) than a number of other well-known oxides [8]. Y_2O_3 has a wide energy band gap, high electrical resistivity range (10^{11}-10^{12}ohm/m), dielectric permittivity (11-15), and electric strength (10^8-10^9 Vm^{-1}); it also shows low dielectric losses (0.01-0.03) and good transparency in a wide spectral range with little light diffusion [9 - 12]. Due to these properties, Y_2O_3 is a prospective material for antireflection and protective coatings, interference mirrors and for manufacturing passive components and dielectric layers in multilevel integrated circuits [10]. Much attention, therefore, has been paid to Y_2O_3 nanomaterials for memory devices owing to their electrical characteristics and potential applications [13].

The structural and optical properties of stoichiometric Y_2O_3 have been studied theoretically and the effect of neutral oxygen vacancies on the electronic structure of Y_2O_3 has been investigated earlier [14 – 17]. Hence an attempt is made to study the influence of bismuth dopant and the doping concentration on the structural and optical properties of yttrium oxide, as a host lattice.

Yttrium oxide was prepared by sputtering [18], photo ablation [19], solution combustion technique [20, 21], magnetron sputtering [22 - 25], ion beam sputtering [26], wet chemical method [27], catalyst enhanced Chemical vapour deposition [28], sol- gel method [29], precursor-templated conversion method [30], hydrothermal method of different precursors [31], sol-gel method [32] and were reported earlier. The absorption and emission transitions of phosphors activated with ions with ns^2 configuration (e.g., Bi^{3+} activated phosphors) are strongly dependent on the host lattice; although they have been extensively investigated, there are few reports on the luminescent characteristics of Bi- activated oxide phosphors [33].

Bi^{2+}-doped MBPO$_5$ (M = Ba^{2+}, Sr^{2+}, Ca^{2+}) synthesized in air via solid state reaction, by Peng et al [33], and are considered as novel orange and red phosphors for white light emitting diodes with improved colour quality. Absorption of Bi^{2+} due to $^2P_{1/2} \rightarrow ^2S_{1/2}$ and $^2P_{1/2} \rightarrow ^2P_{3/2}$ could be observed and quantified by them.

The irradiation effect on bismuth doped CaS nanocrystalline phosphors and their possible applications to solid state dosimetry have been studied by Kumar et al [35]. The wet chemical co-precipitation method has been used for preparation of nanocrystallites.

Bi^{2+}-doped BaSO$_4$ phosphor was synthesized in air by Cao [36] via solid state reaction method. Three excitation bands and one emission band were observed at 260 nm ($_2$P$^{1/2} \rightarrow _2$S$^{1/2}$), 452 nm ($_2$P$^{1/2} \rightarrow _2$P$^{3/2}$(2)), 592 nm ($_2$P$^{1/2} \rightarrow _2$P$^{3/2}$(1)), and 627 nm ($_2$P$^{3/2}$(1) $\rightarrow _2$ P$^{1/2}$), respectively. W-LEDs were demonstrated by using a blend composition of BaSO$_4$:Bi^{2+} and YAG: Ce^{3+} phosphors pumped with a 455 nm blue LEDs chip. The results indicate that BaSO$_4$:Bi^{2+} phosphor is suitable as potential red phosphor for application in W-LEDs excited with blue LEDs chip.

Precipitation methods of preparation of yttrium oxide samples other than sol-gel method are reported less. Also

among the dopants europium and other rare earth dopants are reported more. Even in sol-gel method, the precipitating reagents are not given that much importance. Bismuth doped yttrium oxide are rarely prepared by simple precipitation methods, also by using different precipitating agents and of different doping concentration.

Hence in this paper, the preparation of bismuth (on the basis of ionic size Bi^{3+} (radius -~ 0.96Å) is very close to Y^{3+} (r -~ 0.92Å) [37] doped yttrium oxide samples of three different doping concentration by simple precipitation techniques like sol-gel, solvothermal and wet chemical method by using different precipitating agents like ammonium hydroxide, sodium hydroxide and oxalic acid has been reported and the complete analysis of their optical and structural properties are done.

2. Experimental details

Pure Yttrium Oxide, Bismuth doped yttrium oxide samples of three different concentrations, 0.25, 0.5 and 1 weight percentage of yttrium precursor are prepared by sol-gel, solvothermal and wet chemical method. Yttrium nitrate hexahydrate is used as the yttrium precursor; bismuth nitrate is used as the bismuth dopant precursor

2.1 Sol-gel method

To prepare pure sample, A Pure, 1 g of Yttrium nitrate hexahydrate ($Y(NO_3)_3.6H_2O$) was dissolved in 10 ml of distilled water and stirred for long time to dissolve the salt completely, followed by ammonium hydroxide, the precipitating agent, added in drops to get a clear solution. Continuous stirring lead to precipitation and the precipitate was left for 15 hours to settle. Then the obtained precipitate was washed with water and dried in an oven at 373 K for 3 hours. After drying, the powder was finely ground. Calcination was done by heating the sample at 623 K in a muffle furnace for 15 hours to obtain pure yttrium oxide [32]. To prepare bismuth doped yttrium oxide powders AB1, AB2 and AB3, 1 g of Yttrium nitrate hexahydrate was dissolved in 10 ml of distilled water and stirred for long time to dissolve the salt completely. Then bismuth nitrate of 0.25, 0.5 and 1 weight percentage of yttrium precursor respectively were added to the solution followed by the addition of 50 ml of ammonium hydroxide. Continuous stirring lead to precipitation and the precipitate was left for 15 hours to settle. Then the obtained precipitate was washed with water and dried in an oven at 373 K for 3 hours. After drying, the powder was finely ground. Calcination is done by heating the sample at 623 K in a muffle furnace for 15 hours to obtain doped yttrium oxide powder [32].

2.2 Solvothermal method

In this method, pure yttrium oxide, B Pure was prepared by dissolving 0.6 g of Yttrium Nitrate hexahydrate $Y(NO_3)_3.6H_2O$ in 160 ml of absolute ethanol under stirring to dissolve the salt completely. 6.4 g of sodium hydroxide solid which acts as a precipitating agent was dropped into these solutions. Then 30 minutes of vigorous stirring was continued. After that the samples were heated at 433 K for 3 hours in an oven and cooled to room temperature. The white powder formed at the bottom was washed with ethanol and distilled water several times to remove any possible remnants. Finally the product, B Pure was dried at 353 K in an oven for 2 hours [38].

Bismuth doped yttrium oxide samples BB1, BB2 and BB3 were prepared by dissolving 0.6 g of Yttrium Nitrate hexahydrate $Y(NO_3)_3.6H_2O$ in 160 ml of absolute ethanol under stirring to dissolve the salt completely. 6.4 g of sodium hydroxide solid which acts as a precipitating agent was dropped into those solutions followed by the addition of bismuth nitrate (0.25, 0.5 and 1 weight percentage of yttrium precursor). Further 30 minutes of vigorous stirring was continued. After that the samples were heated at 433 K for 3 hours in an oven and cooled to room temperature. The white powder formed at the bottom was washed with ethanol and distilled water several times to remove any possible remnants. Finally the products were dried at 353 K in an oven for 2 hours [38].

2.3 Wet chemical method

The preparation of pure yttrium oxide, C Pure by wet chemical method was done by involving a precipitation reaction between the yttrium nitrate hexahydrate with oxalic acid as a precipitant agent. Precipitation was conducted at 353 K in an oven, Yttrium nitrate solution (0.6 g) was added together with oxalic acid (0.9 g) into diluted solution of oxalic acid (1:10) to prepare pure sample. The precursor post precipitation stage consists of washing and drying [27].

The preparation of bismuth doped yttrium oxide samples CB1, CB2 and CB3 by wet chemical method was done by involving a precipitation reaction between the yttrium nitrate hexahydrate with oxalic acid as a precipitant agent and the bismuth nitrate. Precipitation was conducted at 353 K in an oven. Yttrium nitrate solution was added together with oxalic acid into diluted solution of oxalic acid (1:10), dopant concentration of 0.25, 0.5 and 1 weight percentage of yttrium precursor were added to the resulting solutions to get the bismuth doped yttrium oxide samples. The precursor post precipitation stage consists of washing and drying [27].

2.4 Characterisation

The powder XRD study is carried out using a Shimadzu XRD 6000 X-ray diffractometer using CuKα radiation. The morphological investigation of the bismuth doped yttrium oxide nanoparticles are performed in JEOL Model JSM - 6390LV Scanning Electron Microscope. Elemental analysis of the samples is done by EDAX EOL Model JED – 2300 make to determine the presence and percentage of bismuth, yttrium and oxygen ions. The UV-Visible spectra for the samples are taken using JASCO UV-Vis- NIR spectrophotometer (Model V-570) in the wavelength range 200 to 1200nm. The photoluminescence spectrum is obtained by using FLUOROLOG, HORIBA YVON spectrophotometer.

3. Results and discussion

3.1 FTIR

Fig. 1(a), (b) and (c) shows FTIR spectra of pure yttrium oxide and bismuth doped yttrium oxide samples of three different dopant concentrations prepared by sol-gel, solvothermal and wet chemical methods by using three different precipitating agents Ammonium hydroxide, Sodium hydroxide and oxalic acid respectively. Infrared studies were carried out in order to ascertain the purity and nature of the samples. Transition metal oxides generally give absorption bands in fingerprint region i.e. below 1000 cm^{-1} arising from inter-atomic vibrations. The transition metal-oxygen frequencies observed for the respective metal oxides are in accordance with literature values [39, 40].

Fig. 1 (a) show the FTIR spectra of pure yttrium oxide and bismuth doped yttrium oxide samples prepared by sol-gel method of three different dopant concentrations by using ammonium hydroxide as precipitating agent. The band centred within the range 560 -700 cm^{-1} is attributed to Y–O stretching mode of Y_2O_3 structure [41]. The absorption band of O - H stretching vibrations appears within the range 3300 -3400 cm^{-1} and around 1600cm^{-1} which shows that more absorption of water occurs with increase in dopant concentration. And both the bands undergo broadening with dopant concentration. The band within the range 740 – 990 cm^{-1} corresponds to Bi-O stretching. The band around 1400 cm^{-1} is attributed to O-H bending [42] and it is observed that there is both broadening of band and shift in band with respect to dopant concentration. Although efforts are made to limit sample exposure to humidity, it is likely that samples adsorb traces of moisture during transfer from the sample box to the FTIR sample chamber, resulting in some hydrolysis [43] (Liu et al 1996). Sharpening of band occurs around 740 – 990 cm^{-1} with increasing dopant concentration, shows the effect of bismuth concentration in the structure.
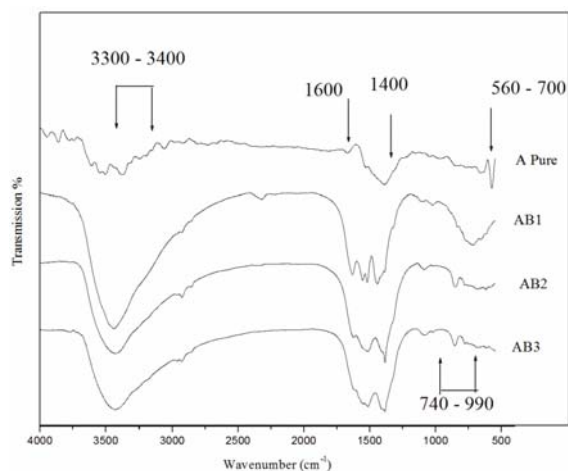

Fig. 1. (a) FTIR spectra of pure yttrium oxide and bismuth doped yttrium oxide samples prepared by sol-gel method.

Fig. 1(b) shows the FTIR spectra of pure yttrium oxide and bismuth doped yttrium oxide samples of three different dopant concentrations prepared by solvothermal method by using sodium hydroxide as precipitating agent. It shows similar response as samples prepared by sol-gel method.
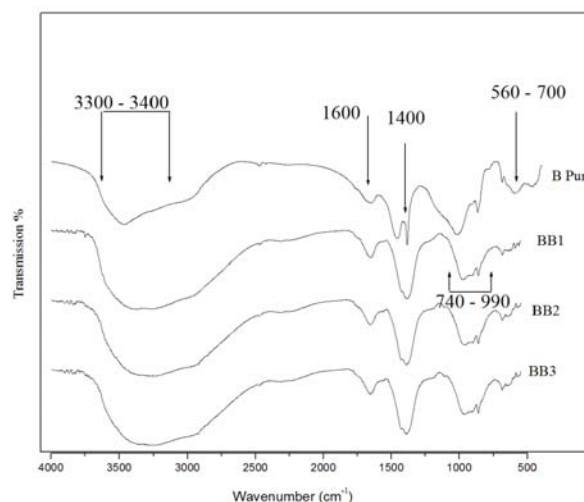

Fig. 1 (b) FTIR spectra of pure yttrium oxide and bismuth doped yttrium oxide samples prepared by solvothermal method.

Fig. 1 (c) shows the FTIR spectra of pure yttrium oxide and bismuth doped yttrium oxide samples of three different dopant concentrations prepared by wet chemical method by using oxalic acid as precipitating agent. It shows similar response as samples prepared by sol-gel method except with some distortion, which may be due to the difference in preparation technique.
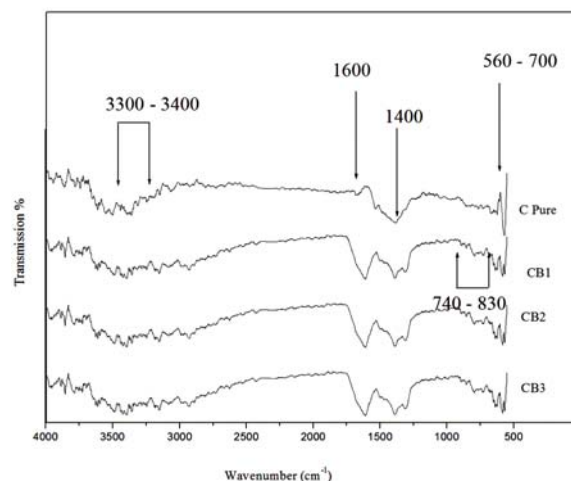

Fig. 1. (c) FTIR spectra of pure yttrium oxide and bismuth doped yttrium oxide samples prepared by wet chemical method

From the analysis of FTIR studies, it has been observed that both the dopants and the preparation techniques affect the properties of the samples.

3.2 Structural studies

Structural analysis of the samples were done by XRD, SEM and EDAX studies

3.2.1 XRD

XRD pattern of pure yttrium oxide and bismuth doped yttrium oxide samples of three different dopant concentrations prepared by sol-gel method, solvothermal method and wet chemical method by using Ammonium hydroxide, sodium hydroxide and oxalic acid as precipitating agents respectively are shown in figs. 2 (a), (b) and (c). Table 1 lists the details of composition and calculated crystallite sizes of pure yttrium oxide and bismuth doped yttrium oxide samples estimated from the well-defined known Debye - Scherrer's equation [44].

From fig. 2 (a) of XRD pattern of pure yttrium oxide and bismuth doped yttrium oxide samples prepared by sol-gel method it is observed that the structure of the pure sample shows amorphous nature with hump around 30° and emerging peaks around 27° and 48.5°. It has been observed that the doped samples show amorphous nature with emerging peaks characteristic of Monoclinic (JCPDS 391063) structure of yttrium oxide, which is enhanced due to doping and it is mixed with amorphous nature. The emerging peaks show that the samples started to crystallize. It is also observed that the crystallinity increases with doping concentration but with higher doping concentration (1 weight percentage) the crystallinity decreases, since at the higher dopant concentration, the structural deformation produced by the dopant in the host lattice is more. Hence with the increasing dopant concentration, crystallinity and crystallite size of the yttrium oxide particles decreased gradually [45].
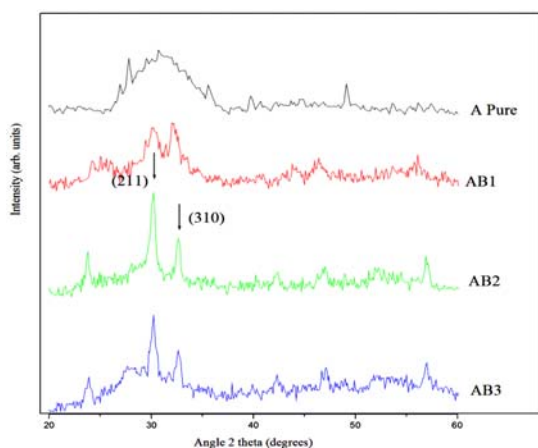

Fig. 2. (a) XRD pattern of pure yttrium oxide and bismuth doped yttrium oxide samples prepared by sol-gel method.

From fig. 2 (b) of XRD pattern of pure yttrium oxide and bismuth doped yttrium oxide prepared by solvothermal method, it is observed that the pure sample has amorphous nature with broad hump and has emerging diffraction peaks around 29°, 43 ° and 52 °which show that the samples started to crystallize. The doped samples show diffraction peaks characteristic of Monoclinic (JCPDS 471274) structure of yttrium oxide with more or less similar particle size and improved crystallinity with doping and dopant concentration. It is observed that the doped samples show better crystalline nature than the pure

one, though amorphous nature is also present in it. It has been observed that with higher doping concentration of 1 weight percentage, the doped samples show decrease in crystallinity, with the same reason explained for sol-gel method.
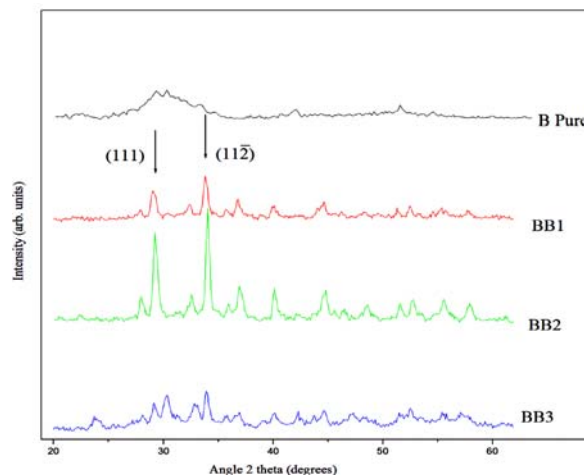

Fig. 2. (b) XRD pattern of pure yttrium oxide and bismuth doped yttrium oxide samples prepared by solvothermal method.

Fig. 2 (c) XRD pattern of pure yttrium oxide and bismuth doped yttrium oxide prepared by wet chemical method shows that pure sample shows peaks characteristic of Monoclinic Primitive (JCPDS 391063) structure of yttrium oxide with highest peak around 31° due to the diffraction along (202) plane and shows somewhat better crystalline nature. When compared with pure sample though the structure is same, shift in peaks are observed in the doped samples due to the distortion in the crystal structure created by the introduction of the bismuth dopant [46]. Also it is found that the sample with higher doping concentration shows more shift in peaks with amorphous nature which may be attributed to the high concentration of dopant which distorts the lattice more due to difference in ionic size of bismuth and yttrium and also it shows more crystallinity which is also due to the higher dopant concentration [47, 45].
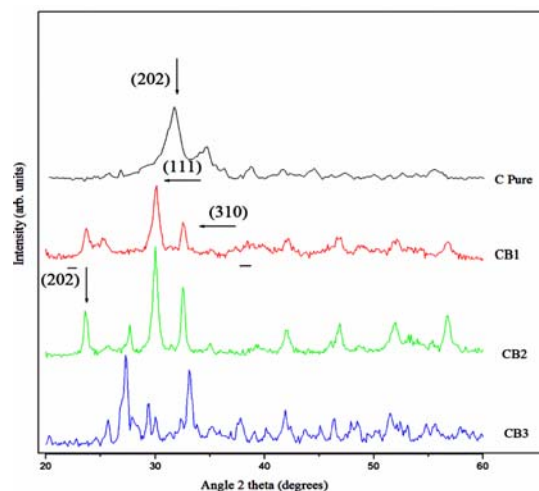

Fig. 2. (c) XRD pattern of pure yttrium oxide and bismuth doped yttrium oxide samples prepared by wet chemical method.

It is observed from the XRD analysis that the samples prepared by wet chemical method using oxalic acid as precipitating agent shows better crystalline nature both in pure and doped sample, which may be due to the drying process, low temperature adopted in this method. In case of doped samples prepared by solvothermal, and sol-gel method crystallinity initially increases then decreases with doping concentration. It is observed in all the three methods that the doping increases crystallinity nature and also the crystallinity increases with doping concentration and then it has been suppressed at higher doping concentration of 1 weight percentage. Though the materials prepared have same composition, their structure differs due to the difference in method followed for preparation.

It has been found that the doped Bi ions had little influence on the host Y_2O_3 structure. Also it is observed that the bismuth doping increased the lattice parameters of the samples, due to the fact that the ionic radius of Y^{3+} (0.092 nm) are slightly lower than Bi^{3+} (0.096 nm). Thus, the shifting of peak position to lower angle with increase in dopant concentration in the XRD studies indicates the expansion of lattice parameters [48]. Bi^{3+} ions are expected to occupy the Y^{3+} sites in this material. Strain is induced in the yttrium oxide lattice due to the substitution of Bi^{3+} ions by comparatively higher ionic radius of ions [49, 50].

Table 1. Details of composition and calculated crystallite size of samples from XRD of pure yttrium oxide and bismuth doped yttrium oxide samples

Sample	Composition	Crystallite size (nm)
AB1	Y_2O_3:Bi (0.25 Weight % of Yttrium precursor)	19.5
AB2	Y_2O_3:Bi (0.5 Weight % of Yttrium precursor)	11.39
AB3	Y_2O_3:Bi (1 Weight % of Yttrium precursor)	12.3
BB1	Y_2O_3:Bi (0.25 Weight % of Yttrium precursor)	17
BB2	Y_2O_3:Bi (0.5 Weight % of Yttrium precursor)	17
BB3	Y_2O_3:Bi (1 Weight % of Yttrium precursor)	22.2
C Pure	Y_2O_3	14.62
CB1	Y_2O_3:Bi (0.25 Weight % of Yttrium precursor)	11.52
CB2	Y_2O_3:Bi (0.5 Weight % of Yttrium precursor)	14.61
CB3	Y_2O_3:Bi (1 Weight % of Yttrium precursor)	12.53

3.2.2 SEM

All the SEM images of pure yttrium oxide and bismuth doped yttrium oxide samples of three different dopant concentration prepared by sol-gel, solvothermal and wet chemical method by using ammonium hydroxide, (A Pure, AB1, AB2, AB3), sodium hydroxide (B Pure, BB1, BB2, BB3), and oxalic acid (C Pure, CB1, CB2, CB3) as the precipitating agents respectively are shown in figures 3, 4 and 5. The precipitating reagents and the method of preparation of samples have influenced the morphology and crystallite size of pure and bismuth doped yttrium oxide samples which have been illustrated in the SEM images.

Fig. 3 (a), (b), (c) and (d) show the SEM images of pure yttrium oxide and bismuth doped yttrium oxide samples of three different dopant concentration prepared by sol- gel method. Pure yttrium oxide sample shows the cumulative nature of secondary particl es which are made up of agglomeration of many primary particles. The obtained particles do not have a uniform shape and size as obtained from SEM micrographs. The Y_2O_3 particles exhibit agglomeration because of the dipole interaction [51]. In Doped samples it can be observed that all the powder fractions have irregular morphology. It could have been originated by the coalescence of almost spherical particles with several sizes and the bismuth doped yttrium oxide sample with 1 weight percentage shows is similar to

as shown by Fu et al [52] that it is the common morphology of bismuth samples [53].
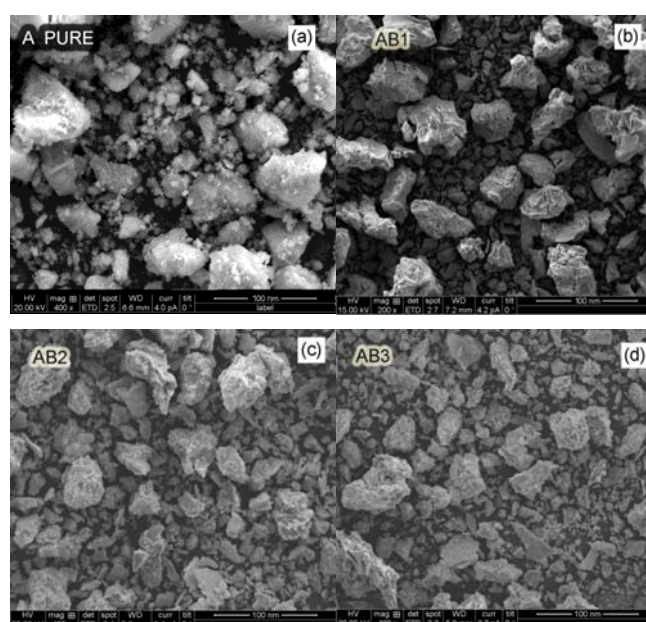

Fig. 3.(a), (b), (c) and (d) SEM images of pure yttrium oxide and bismuth doped yttrium oxide samples prepared by sol- gel method.

Fig. 4 (a), (b), (c) and (d) show the SEM images of pure yttrium oxide and bismuth doped yttrium oxide samples of three different dopant concentration prepared by solvothermal method. Pure yttrium oxide sample shows the cumulative nature of secondary particles which are made up of agglomeration of many primary particles. Also it shows irregular grains of mean sizes 15± 5 nm. It clearly shows that the particles are formed in spheroid shape. There are very small agglomerated particles and this might be due to the lower calcination temperature [46]. SEM images of Bismuth doped yttrium oxide samples show agglomeration of samples. Although some other shapes were observed, the main morphology of the product was triangular. Fu et al [52] suggested a possible mechanism of the growing process of triangular bismuth. Growth rates of the different faces were quite different and the bismuth particles could grow towards a preferential direction with the influence of various factors to form triangular plates [52, 53].
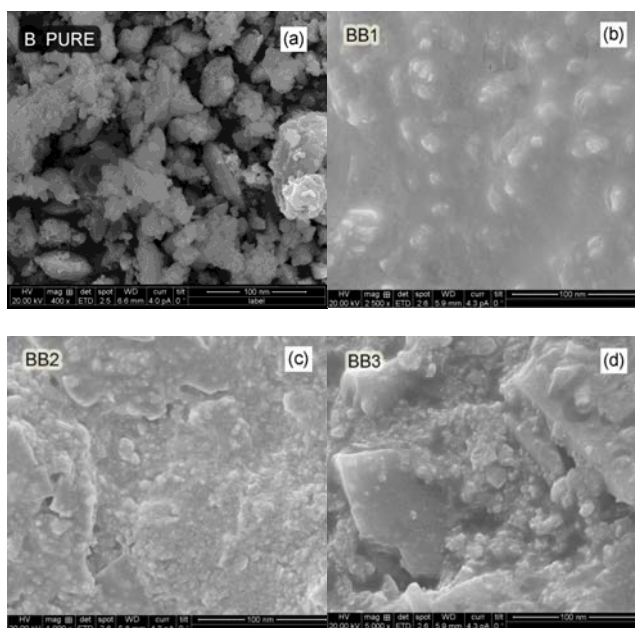
method, the high concentration of yttrium ions may lead to the burst of the initial homogeneous nucleation and then the super saturated yttrium oxide nuclei fond to aggregate together to decrease the surface energy. As the reaction proceeded the concentration of the yttrium oxide became lower and some active sites on the surface of the initially formed yttrium oxide aggregations would grow along the oriented direction. The preferential growth along the oriented directions resulted in yttrium oxide nanoflakes on the surface of the initially formed yttrium oxide aggregation [57]. As a result, 3 D flower like yttrium oxide nanoflakes have been prepared in the present reaction system. And the SEM images of bismuth doped yttrium oxide samples show triangular shape as reported by Hwanga et al [53] and Fu et al [52].
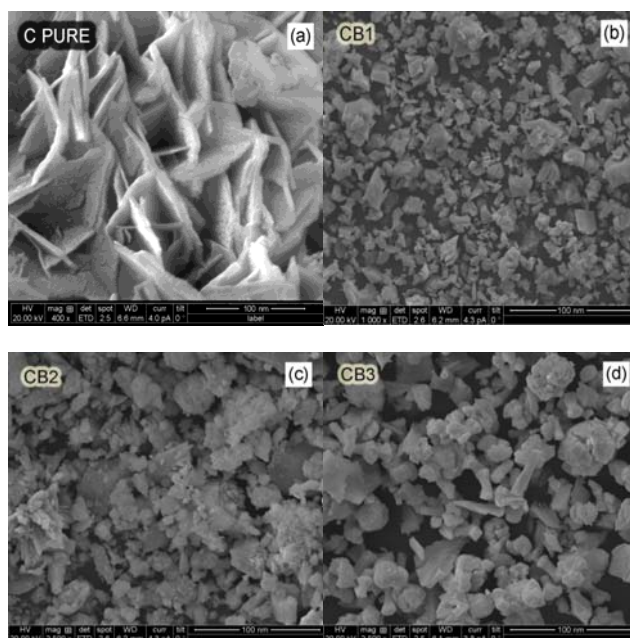

Fig.4. (a), (b), (c) and (d) SEM images of pure yttrium oxide and bismuth doped yttrium oxide samples prepared by solvothermal method.

Fig. 5.(a), (b), (c) and (d) SEM images of pure yttrium oxide and bismuth doped yttrium oxide samples prepared by wet chemical method.

Fig. 5 (a), (b), (c) and (d) show the SEM images of pure yttrium oxide and bismuth doped yttrium oxide samples of three different dopant concentration prepared by wet chemical method. SEM images of the pure yttrium oxide sample shows that the yttrium oxide is composed of 3D flower like microstructures with diameter in the range of 50-60 nm.   Regarding the formation of 3D flower like yttrium oxide nanopowders, the discussion may be proposed as analysed by Peng et al [53] which is discussed follows. It is well known that the shape control of the nanocrystals can be achieved by manipulating the growth kinetics [54 - 56]. In the present case of preparation

Depending upon the precipitating agent used in the synthesis, the morphology of the sample varies. This may be due to the difference in ionic strength of the solution. It is observed from the SEM images of pure yttrium oxide and bismuth doped yttrium oxide of three different dopant concentration prepared by sol-gel, solvothermal and wet chemical method that pure sample prepared by sol-gel and solvothermal methods show irregular grains of different sizes and that prepared by wet chemical method shows flower like structure due to growth kinetics. Doped samples prepared by all the three methods show mainly triangular morphology. It is also observed that crystallite size decreases with dopant concentration. Hence it can be identified that the preparation technique affects the morphology of the samples.

3.2.3 EDAX

EDAX spectrum of the samples of pure yttrium oxide and bismuth doped yttrium oxide prepared by sol-gel, solvothermal and wet chemical method of three different doping concentration by using ammonium hydroxide, (A Pure, AB1, AB2, AB3), sodium hydroxide (B Pure, BB1, BB2, BB3), and oxalic acid (C Pure, CB1, CB2, CB3) as the precipitating agents are shown in figs. 6 and 7.

From the EDAX spectrum of pure yttrium oxide samples prepared by sol-gel, solvothermal and wet chemical method as given in fig. 3.6 (a), (b), and (c) the presence of the characteristic and distinct line of yttrium (L) and Oxygen (K) have been identified. In the sample A pure, prepared by sol-gel technique, the percentage of oxygen is found to be 5 and that of yttrium is 87. Similarly in the sample B prepared by solvothermal method, percentage of oxygen is 14 and that of yttrium is 64. In the sample C, prepared by wet chemical method, the oxygen content is found to be 9 and yttrium is 73.
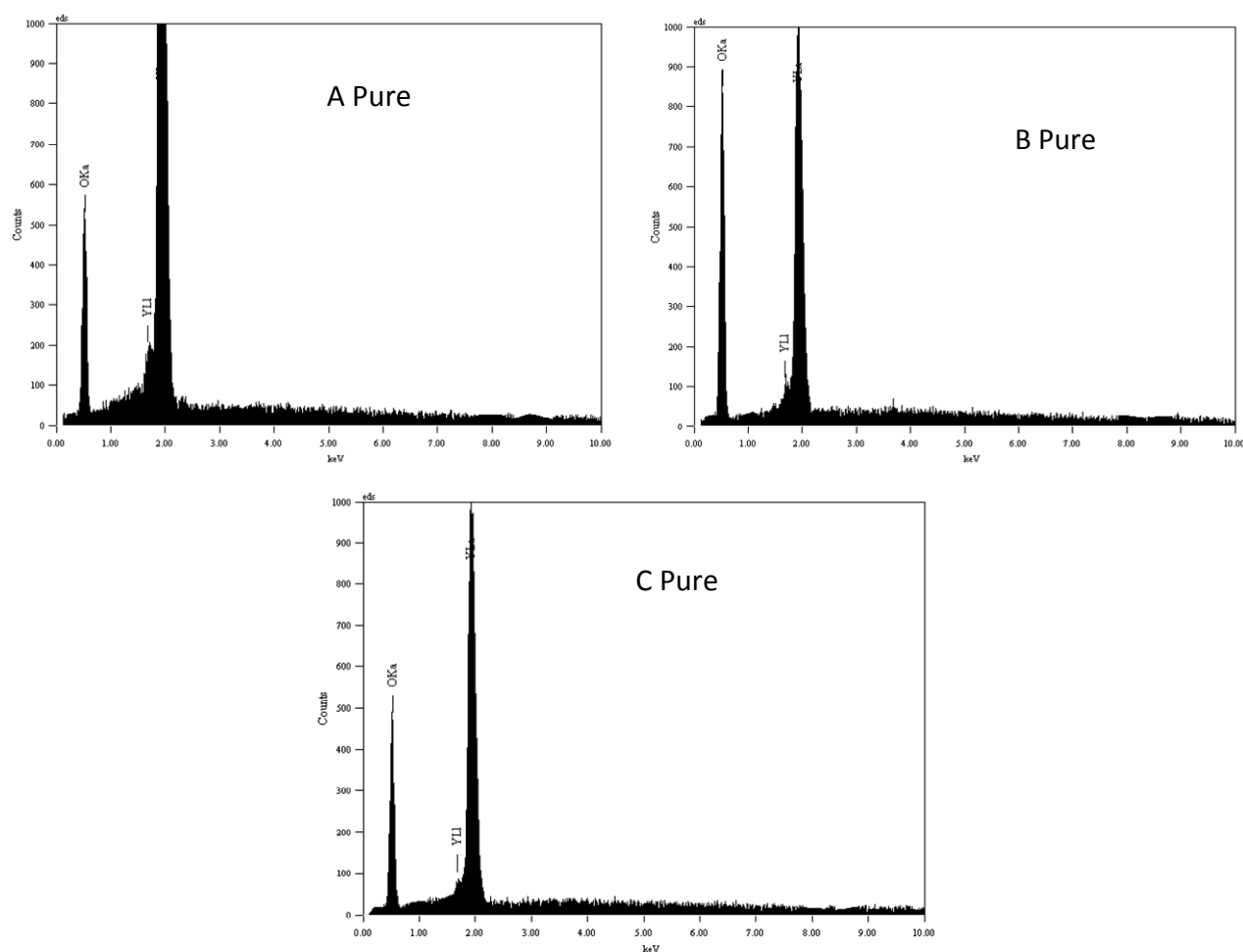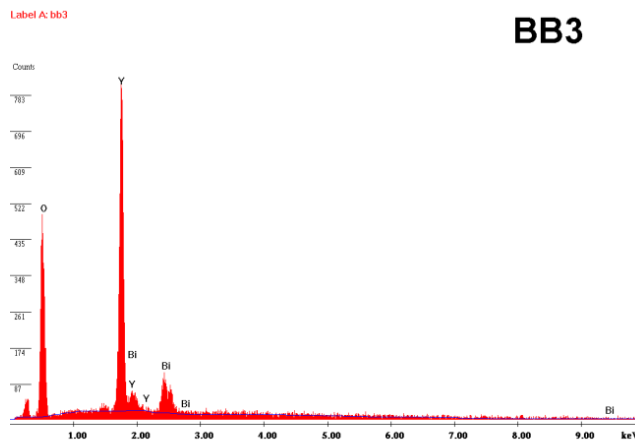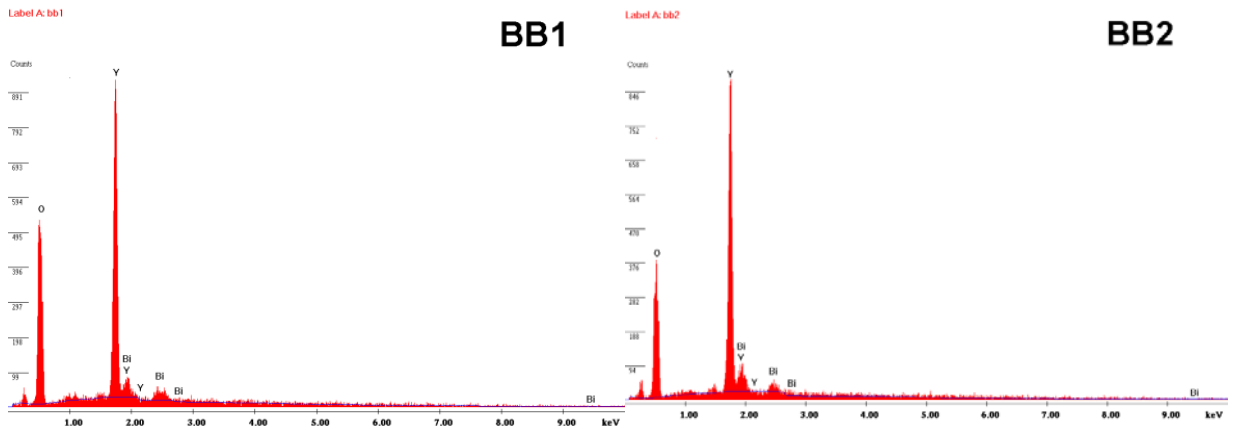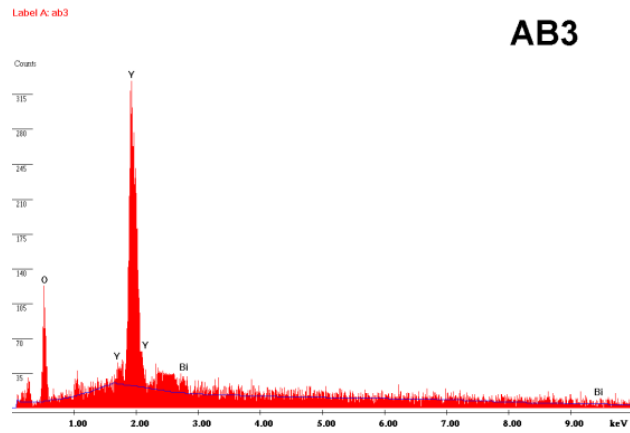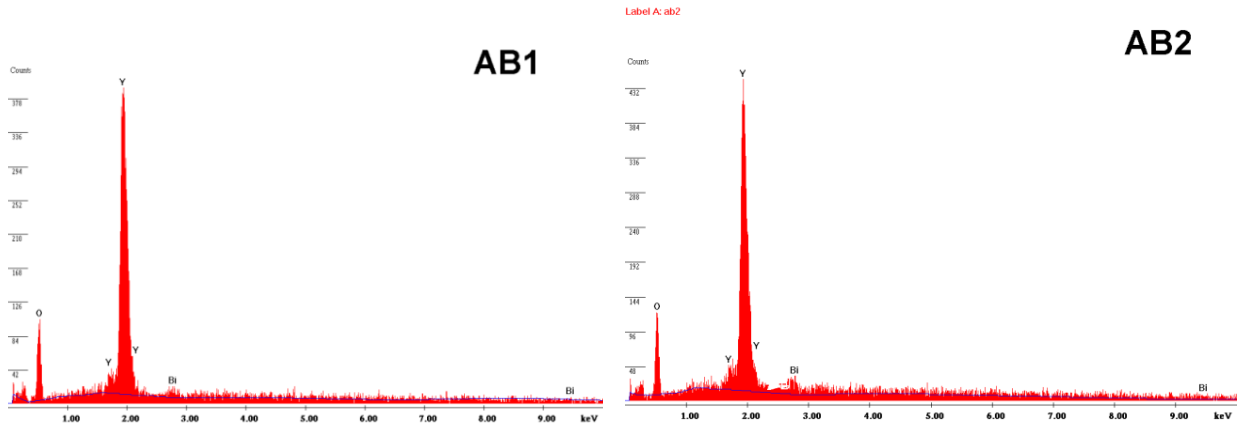

Fig. 6. EDAX spectrum of elemental analysis of the pure yttrium oxide samples prepared by (a) Sol-Gel method, (b) Solvothermal method and (c) Wet chemical method.

Fig. 7 gives the EDAX spectrum of the bismuth doped yttrium oxide prepared by sol-gel, solvothermal and wet chemical method of three different dopant concentration by using ammonium hydroxide, (AB1, AB2, AB3), sodium hydroxide (BB1, BB2, BB3), and oxalic acid (CB1, CB2, CB3) as the precipitating agents, the presence of the characteristic and distinct spectral line of yttrium, Bismuth and Oxygen have been identified. From the fig. 7 it is observed that the weight percentage of bismuth varies between 4 and 5 for the samples prepared by sol-gel method and for the samples prepared by solvothermal method it varies between 1 and 3 and for wet chemical method the range is between 3 and 7.

AB1

AB2
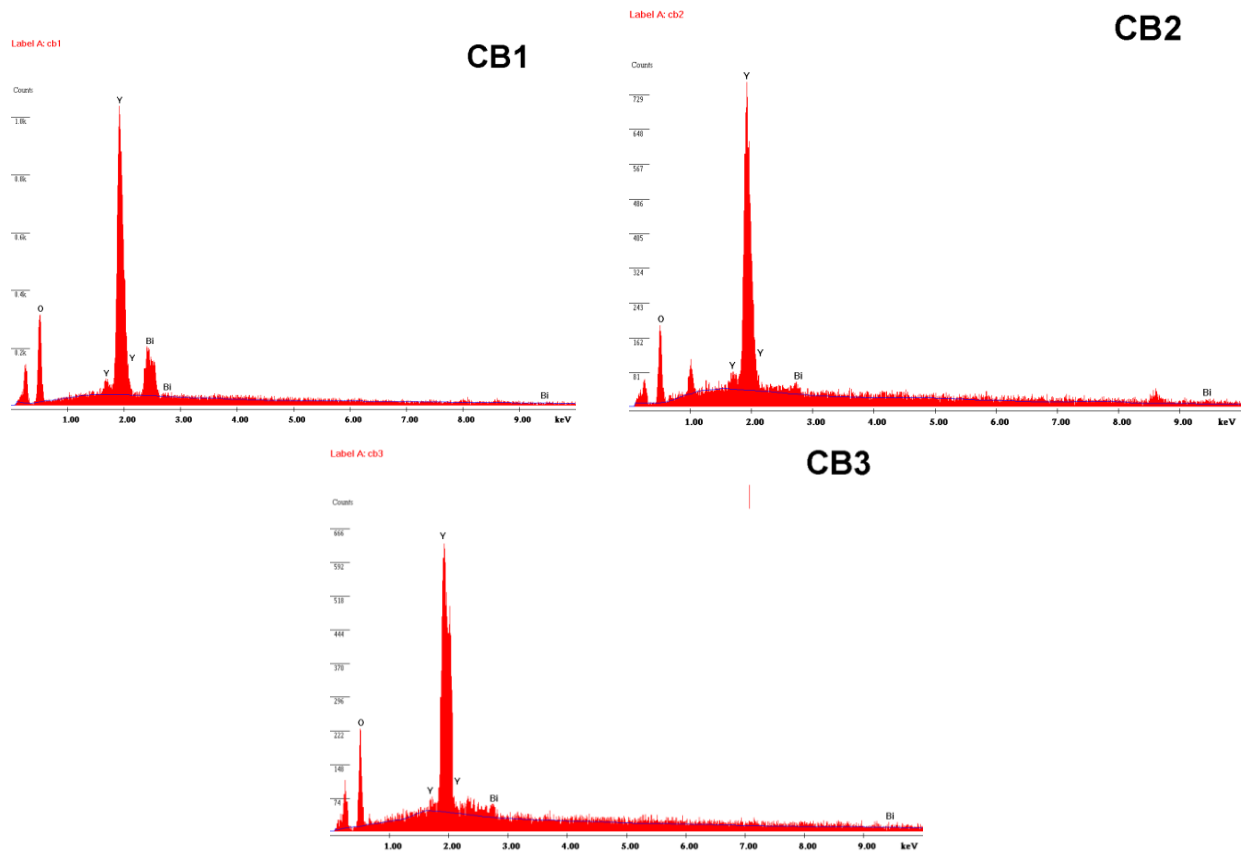
AB3

BB1

BB2

BB3

Fig.7. EDAX spectrum of elemental analysis of the bismuth doped Yttrium Oxide samples prepared by sol-gel method, solvothermal method and wet chemical method.

It can be observed that, in the samples, the real dopant concentration is higher than the calculated value, thus illustrating that the precipitation of dopant and yttrium is achieved with variable rates. The fact that the difference between the determined and experimental values does not show a monotonous evolution trend illustrates the complexity of the precipitation process. The formation of sample is influenced by both the solubility of dopant and yttrium precursor and the precipitation agent used [27].

3.2.4 Optical studies

Analysis of optical properties of the samples were done by UV visible absorption studies and PL studies.

3.2.4.1 UV visible absorption studies

The UV-Visible absorption spectrum of pure yttrium oxide and bismuth doped yttrium oxide samples prepared by sol-gel, solvothermal, and wet chemical method by using ammonium hydroxide, sodium hydroxide and oxalic acid as precipitating agents of three different dopant concentration are shown in figures 8 (a), (b) and (c) and the band gap energy estimated from UV visible absorption studies [58] is tabulated in table 2.
From the UV visible absorption spectrum of pure and bismuth doped yttrium oxide samples of three different dopant concentration prepared by sol-gel method using ammonium hydroxide as a precipitating agent shown in figure 8 (a) it is observed that the pure sample shows peak only around 200 nm which is due to the absorption of

yttrium oxide [59]. And the bismuth doped yttrium oxide samples show absorption around 300 nm due to Surface Plasmon Resonance (SPR).
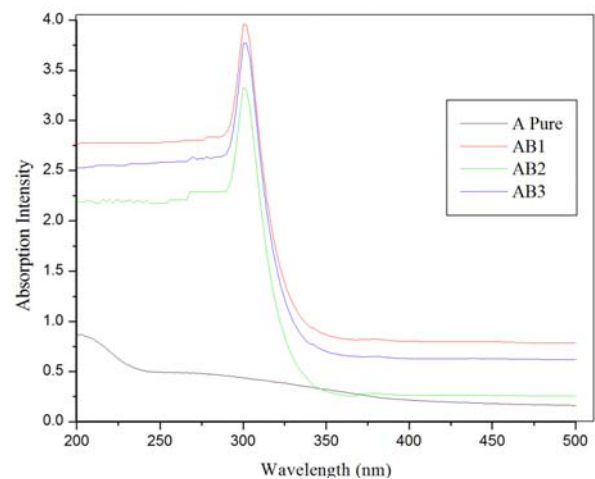

Fig. 8. (a) UV visible absorption of pure yttrium oxide and bismuth doped yttrium oxide samples prepared by sol-gel method.

As stated earlier by Singh & Karmakar [60], when the wavelength of light is much larger than the nanoparticle size it can set up standing resonance conditions. Light in resonance with the surface Plasmon oscillation causes the free-electrons in the metal to oscillate. As the wave front of the light passes, the electron density in the particle is polarized to one surface and oscillates in resonance with

the light's frequency causing a standing oscillation. The resonance condition is determined from absorption and scattering spectroscopy and is found to depend on the shape, size, and dielectric constants of both the metal and the surrounding material. This is referred to as the Surface Plasmon Resonance (SPR), since it is located at the surface. As the shape or size of the nanoparticle changes, the surface geometry changes which cause a shift in the electric field density on the surface. This causes a change in the oscillation frequency of the electrons, generating different cross-sections for the optical properties including absorption and scattering. Bismuth doped yttrium oxide samples show strong absorption around 300 nm, which is being called as surface Plasmon Resonance (SPR) [60]. The SPR band arises due to the interaction of incoming light with the conduction band electrons of the metal. The distortion observed in the lower wavelength region of the spectra is attributed due to the influence of ethanol in which the sample was dissolved for UV-Vis absorption measurements. Also it is observed that with doping concentration initially the absorption intensity decreases and then increases with doping concentration which may be due to the distortion in the host lattice due to the increased dopant concentration. Also pure sample is observed to have less absorption when compared with the doped samples. Both pure and doped samples show no absorption in the visible region. This observation indicates the high-quality and transparent nature of bismuth doped Y_2O_3 samples with almost zero absorption losses. This is very important in order to employ the samples in optical applications, where the absorption losses are kept at minimum.

From the UV visible absorption spectrum of pure yttrium oxide and bismuth doped yttrium oxide samples prepared by solvothermal method using sodium hydroxide as a precipitating agent of three different dopant concentrations shown in figure 8(b), it is observed that the pure sample shows peak only around 200 nm which is due to the absorption of yttrium oxide [59] and the doped samples show similar response with absorption of yttrium oxide around 300 nm as the ones prepared by sol-gel method.
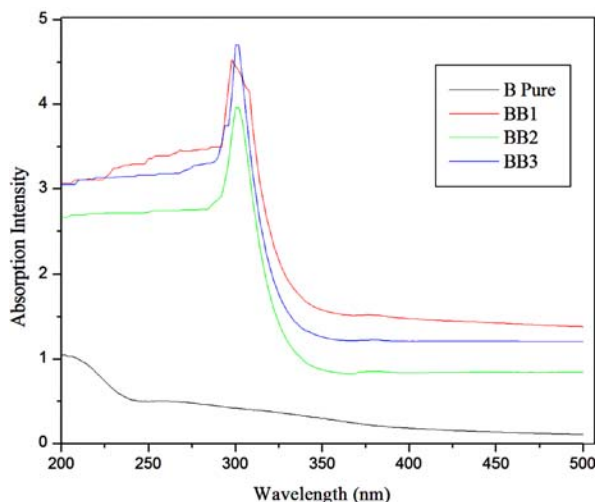

Fig. 8. (b) UV visible absorption of pure yttrium oxide and bismuth doped yttrium oxide samples prepared by solvothermal method.

From the UV visible absorption spectrum of pure yttrium oxide and bismuth doped yttrium oxide samples prepared by wet chemical method using oxalic acid as a precipitating agent of three different dopant concentrations shown in figure 8 (c), it was observed that the pure sample shows absorption around 254 nm which is due to the yttrium oxide and the shift in absorption wavelength may be due to the quantum confinement effect which occurred in the preparation technique adopted for this method like low annealing temperature and the precipitating agent, Oxalic acid. Even SEM images show different morphology of this particular sample. This particular pure sample shows better crystalline than samples. This may be reason for different absorption wavelength, which shows that structure also determines the optical property. The doped samples show absorption around 300 nm which is due to Surface Plasmon Resonance (SPR). In the samples prepared by this method, it was observed that the absorption intensity increases with dopant concentration as expected. This proves that the sample prepared by wet chemical method is the efficient one for absorption studies like optoelectronic devices.
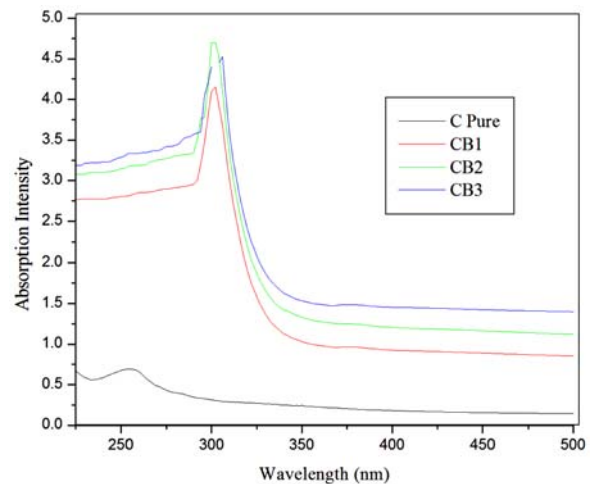

Fig. 8. (c) UV visible absorption of pure and bismuth doped yttrium oxide samples prepared by sol-gel method.

From the estimated band gap energy in table 2 it has been observed that the band gap energy shows red shift with doping. It is due to the formation of impurity band and trapping of bismuth atoms, which leads to the generation of the defect states within the forbidden band [50]. Impurity band formation is an obvious consequence of increased doping concentration [61] and the trapping of the dopant atoms at the grain boundary leads to the introduction of the defect states within the forbidden band. With increasing dopant concentration, density of this dopant induced defect states increases, leading to the observed decrease of band gap or red shift. Actually, trapping of impurities and the introduction of defect states within the forbidden band gap region is intimately related to the disorder introduced in the system by doping. It is quite evident that more disorder should be introduced in the system with increasing dopant concentration as ionic

radius of bismuth is slightly greater than yttrium. Hence band gap energy decreases with dopant concentration.

Table 2. Band gap energy estimated from UV- studies of pure yttrium oxide and bismuth doped yttrium oxide samples.

Sample Name	Band gap Energy (eV)
A Pure	5.17
AB1	3.57
AB2	3.52
AB3	3.46
B Pure	5.28
BB1	3.58
BB2	3.56
BB3	3.54
C Pure	5.3
CB1	3.56
CB2	3.54
CB3	3.52

3.2.4.2 Photoluminescence (PL) studies

The PL emission spectra of bismuth doped yttrium oxide nanophosphors prepared by sol-gel, solvothermal and wet chemical method using ammonium hydroxide, sodium hydroxide and oxalic acid as precipitating agents of three different dopant concentration excited at 300nm are shown in figures 9 (a),(b) and (c). All samples PL measurements were done at room temperature.

It is observed from the figure 9 (a) for the bismuth doped yttrium oxide samples prepared by sol-gel method that the PL emission occurs at two wavelengths around 420 nm and 440 nm and the intensity initially increases then decreases with dopant concentration which is due to concentration quenching. The bismuth activator is added to the host lattice in concentration typically ranging from 0.25 –1% for efficient phosphors. Each phosphor composition has an optimum activator concentration for obtaining maximum luminescence output. This effect is called as 'concentration quenching' and the origin of this effect is thought to be following: Excitation energy is lost from the emitting state due to cross-relaxation, which is called as non-radiative energy transfer, between activators. The optimal activator concentration for a particular phosphor is generally determined empirically. It was found from the PL studies in the bismuth doped yttrium oxide samples prepared by sol-gel method that the dopant concentration of 0.5 weight percentage of yttrium precursor is optimum for luminescence applications.

According to the literature [62], the appearance of two types of emission centers in bismuth doped yttrium oxide samples are due to the placement of Bi^{3+} in two non-equivalent yttrium sites of the Y_2O_3: Bi crystal lattice with $C2$ and $C3i$ symmetry. The blue emission bands are assigned to Bi^{3+} that substitute for Y^{3+} at the site with $C3i$ symmetry; and at the site with $C2$ symmetry. Bordun & Dmitruk [22] investigated luminescence of thin films of Y_2O_3:Bi and indicated that Bi^{3+} in the oxygen environment with $C3i$ symmetry in the Y_2O_3 lattice also produces blue

luminescence with similar spectral properties and an emission maximum at 420nm [63]. However, with increasing concentration of Bi^{3+} ion, the broad band located at 440 nm decreases gradually due to concentration quenching. Also with increase in dopant concentration the small peak around 420 nm is shifted and combined with 440 nm peak to make it broad. This red shift of peak around 420 nm may be caused by different ligand field effect on Bismuth ion [36].
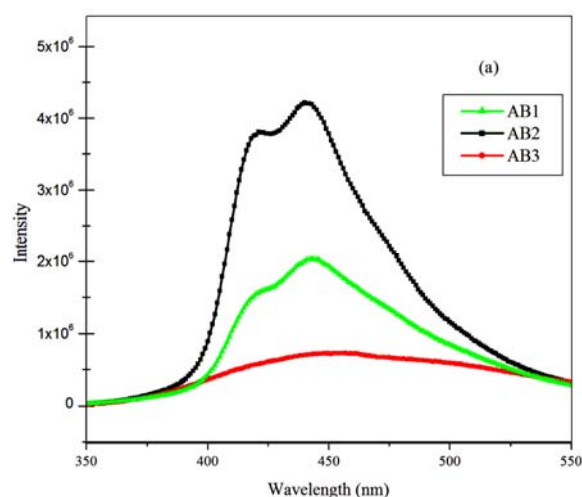

Fig. 9. (a) PL emission of bismuth doped yttrium oxide samples prepared by sol-gel method.

It is observed from the fig. 9 (b) of PL emission of the bismuth doped yttrium oxide samples prepared by solvothermal method by using sodium hydroxide as precipitating agent of three different dopant concentrations that the emission occurs at two wavelengths 420 nm and 440 nm and the intensity initially increases then decreases with doping concentration. The reason for the emission and the difference in emission intensity is the same as discussed for the samples prepared by sol-gel method. However the emission intensity is found to be less when compared with samples prepared by sol-gel method.
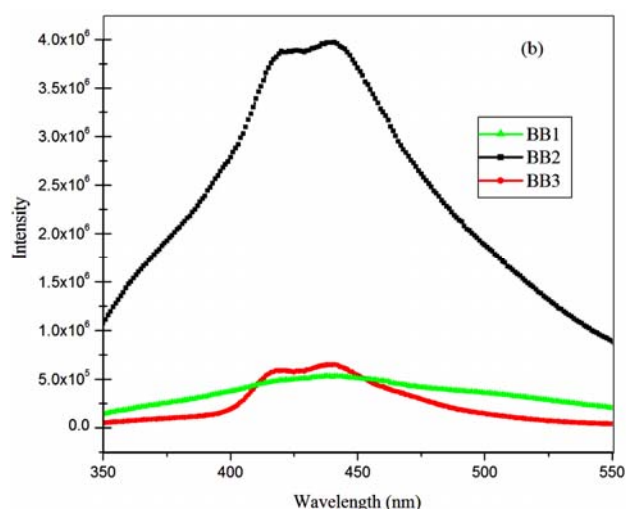

Fig. 9. (b) PL emission of bismuth doped yttrium oxide samples prepared by solvothermal method.

It has been observed from the figure 9(c) of PL emission of bismuth doped yttrium oxide samples prepared by wet chemical method by using oxalic acid as precipitating agent of three different dopant concentrations that the emission occurs at two wavelengths 420 nm and 440 nm and the intensity initially increases then decreases with doping concentration. The reason for the emission and the difference in emission intensity is the same as discussed for the samples prepared by sol-gel method. However it has been observed that the maximum emission intensity is more when compared with both sol-gel and solvothermal method.
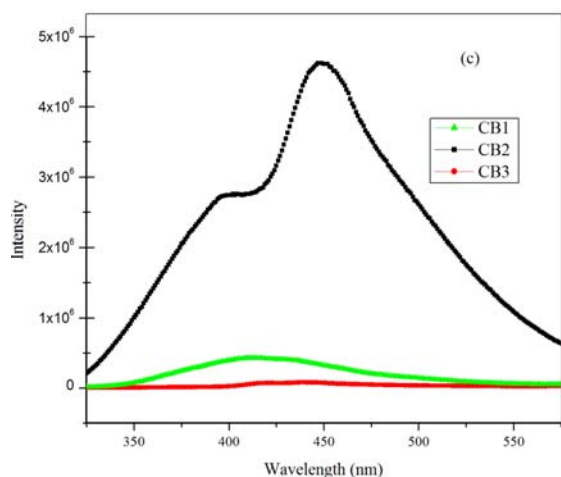

Fig. 9. (c) PL emissions of bismuth doped yttrium oxide samples prepared by wet chemical method.

It was observed from the PL studies of bismuth doped yttrium oxide samples prepared by sol-gel, solvothermal and wet chemical method using ammonium hydroxide, sodium hydroxide and oxalic acid as precipitating agents of three different dopant concentration, that in each method 0.5 weight percentage of yttrium precursor as dopant concentration provides maximum PL efficiency and also it was observed that the sample prepared by wet chemical method has more PL efficiency than other methods. Again this PL study also shows that preparation technique affects the optical properties of the sample.

4. Conclusion

In this paper, structural, elemental and optical properties of pure and bismuth doped yttrium oxide samples prepared by sol-gel, solvothermal and wet chemical method of various dopant concentrations are analysed. FTIR studies represent the formation of functional groups. It was observed from the XRD analysis that the samples prepared by wet chemical method using oxalic acid as precipitating agent show slight crystalline nature both in pure and doped samples, when compared with samples prepared by other methods. It is observed in all the three methods that the doping increases the crystallinity. The crystallinity increases initially with doping concentration then decreases due to lattice distortion. SEM studies show typical morphology of triangular shape for the doped samples and agglomeration

of particles for pure samples prepared by sol-gel and solvothermal method, whereas flower like structure is seen for pure sample prepared by wet chemical method. EDAX studies give the percentage of elements present in the samples. From UV visible studies it was found that the pure samples prepared by sol-gel, solvothermal and wet chemical method show absorption due to yttrium oxide and the doped samples show absorption due to Surface Plasmon Resonance (SPR). Band gap energy estimated from UV studies show that band gap energy decreases with doping due to distortion produced and also the band gap energy decreases with increase in dopant concentration. From PL analysis it was observed that the sample prepared by wet chemical method has more PL emission efficiency than the other samples prepared by other methods. Also most of the doped samples with dopant concentration as 0.5 weight percentage as yttrium precursor has more PL efficiency than the doped samples with other concentration.

References

[1] F. Abraham, M.F. Debreuille-Gresse, G. Mairesse, G. Nowogrocki, Solid State Ionics, **28-30**, 529 (1988).
[2] D.G. Lim, J.H. Lee, J.S. Yi, Structural and electrical properties of a Y 2 O 3 buffer layer by the two step process', 2002.
[3] R. Siegel, Annual Review of Materials Science, **21**(1), 559 (1991).
[4] R. Kodama, Journal of magnetism and magnetic materials, **200**(1), 359 (1999).
[5] Z. Pei, H. Xu, Y. Zhang, Journal of Alloys and Compounds, **468**(1), L5-L8 (2009).
[6] N. Nickel, W. Jackson, J. Walker, Journal of non-crystalline solids, **227**, 885 (1998).
[7] J.Y. Cho, K-Y Ko, Y.R. Do, Thin Solid Films, **515**(7), 3373 (2007)
[8] Ö. Ünal, M. Akinc, Journal of the American Ceramic Society, **79**(3), 805 (1996).
[9] Y-M Wu, J-T Lo, Japanese journal of applied physics, **37**(10R), 5645 (1998).
[10] A. Andreeva, A. Sisonyuk, E. Himich, physica status solidi (a), **145**(2), 441 (1994).
[11] W. Manning, O. Hunter, B. Powell, Journal of the American Ceramic Society, **52**(8), 436 (1969).
[12] C Ling, J. Bhaskaran, W. Choi, L. Ah, Journal of applied physics, **77**(12), 6350 (1995).
[13] M-H Cho, D-H Ko, K Jeong, S. Whangbo, C. Whang, S. Choi, S. Cho, Thin Solid Films, **349**(1), 266 (1999).
[14] F Jollet, C. Noguera, N Thromat, M. Gautier, J. Duraud, Physical Review B, **42**(12), 7587 (1990).
[15] F Jollet, C. Noguera, M. Gautier, N. Thromat, J. P. Duraud, Journal of the American Ceramic Society, **74**(2), 358 (1991).
[16] D. R. Mueller, D. L. Ederer, J. Van Ek, W. L. O'brien, Q. Y. Dong, J. Jia, T. A. Callcott, Physical Review B, **54**(21), 15034 (1996).
[17] Y-N Xu, Z-q Gu, W. Ching, Physical Review B, **56**(23), 14993 (1997).

[18] V. Mudavakkat, M. Noor-A-Alam, K. K. Bharathi, S. AlFaify, A. Dissanayake, A. Kayani, C. Ramana, Thin Solid Films, **519**(22), 7947 (2011).

[19] D. Fried, T. Kushida, G. P. Reck, E. W. Rothe, Journal of applied physics, **73**(11), 7810 (1993).

[20] B. Lakshminarasappa, J. Jayaramaiah, B. Nagabhushana, Powder Technology, **217**, 7 (2012).

[21] J. Mouzon, M. Odén, Powder Technology, **177**(2), 77 (2007).

[22] O. Bordun, V. Dmitruk, Journal of Applied Spectroscopy, **75**(2), 208 (2008).

[23] C. Ramana, V. Mudavakkat, K. K. Bharathi, V. Atuchin, L. Pokrovsky, V. Kruchinin, Applied physics letters, **98**(3), (2011).

[24] D. G. Lim, J. H. Lee, J. S. Yi, Structural and electrical properties of a Y 2 O 3 buffer layer by the two step process. 2002.

[25] R. Ivanic, V. Rehacek, I. Novotny, V. Breternitz, L. Spiess, C. Knedlik, V. Tvarozek, Vacuum, **61**(2), 229 (2001).

[26] M. Jublot, F. Paumier, F. Pailloux, B. Lacroix, E. Leau, P. Guerin, M. Marteau, M. Jaouen, R. Gaboriaud, D. Imhoff, Thin Solid Films, **515**(16), 6385 (2007).

[27] L. Muresan, E. Popovici, E. Indrea, J. Optoelectron. Adv. M., **13**(3), 183 (2011).

[28] Y. Zhang, R.J. Puddephatt, Chemistry of materials, **11**(1), 148 (1999).

[29] R. Mellado-Vázquez, M. García-Hernández, A. López-Marure, P.Y. López-Camacho, Á. de Jesús Morales-Ramírez, H. I. Beltrán-Conde, Materials, **7**(9), 6768 (2014).

[30] H. Manlian, G. Kai, M. Zhenyong, C. Haohong, Y. Xinxin, U. Fangfang, Z. Jingtai, Journal of Rare earths, **29**(9), 830 (2011).

[31] N. Li, K. Yanagisawa, Journal of Solid State Chemistry, **181**(8), 1738 (2008).

[32] R. Subramanian, P. Shankar, S. Kavithaa, S. Ramakrishnan, P. Angelo, H. Venkataraman, Materials Letters, **48**(6), 342 (2001).

[33] H. Fukada, K. Ueda, J-i. Ishino, T. Miyata, T. Minami, Thin Solid Films, **518**(11), 3067 (2010).

[34] M. Peng, N. Da, S. Krolikowski, A. Stiegelschmitt, L. Wondraczek, Optics express, **17**(23), 21169 (2009).

[35] V. Kumar, R. Kumar, S. Lochab, N. Singh, Radiation Effects & Defects in Solids, **161**(8), 479 (2006).

[36] R. Cao, M. Peng, J. Qiu, Optics express, **20**(106), A977 (2012).

[37] R. Datta, Journal of The Electrochemical Society, **114**(11), 1137 (1967).

[38] S. Wang, S. Zhong, X. Ou-Yang, N. Hu, X. Chen, S. Wang, R. Xu, Materials Science and Engineering: B, **162**(3), 200 (2009).

[39] C.N.R. Rao, Chemical applications of infrared spectroscopy, 1963.

[40] I. Markova-Deneva, Journal of the University of Chemical Technology and Metallurgy, **45**(4), 351 (2010).

[41] X. Shen, Y. Zhai, Rare Metals, **30**(1), 33 (2011).

[42] M. Shobana, S. Sankar, Journal of magnetism and magnetic materials, **321**(19), 3132 (2009).

[43] Y. Liu, Z. F. Zhang, B. King, J. Halloran, R. M. Laine, Journal of the American Ceramic Society, **79**(2), 385 (1996).

[44] V. Fruth, A. Ianculescu, G. Voicu, Journal of the European Ceramic Society, **26**(14), 3011 (2006).

[45] M. Pal, U. Pal, J.M.G.Y. Jiménez, F. Pérez-Rodríguez, Nanoscale research letters, **7**(1), 1 (2012).

[46] K. Pandian, Electrical optical and high pressure studies on some transition metals Mn Fe Co Ni Cu Zn and Ce doped SnO2 nanoparticles, Ph.D. thesis, Anna University. 2013.

[47] M. Mallahi, A. Shokuhfar, M. Vaezi, A. Esmaeilirad, V. Mazinani, Am. J. Eng. Res., **3**, 162 (2014).

[48] C. Suryanarayana, M. G. Norton, X-ray diffraction: a practical approach, Springer Science & Business Media, 2013.

[49] P. Singh, A. Kaushal, D. Kaur, Journal of Alloys and Compounds, 471(1), 11 (2009).

[50] R. Karmakar, S. Neogi, A. Banerjee, S. Bandyopadhyay, Applied Surface Science, **263**, 671 (2012).

[51] M. Faisal, S. Khasim, Bulletin of the Korean Chemical Society, **34**(1), 99 (2013).

[52] R. Fu, S. Xu, Y-N Lu, J-J Zhu, Crystal growth & design, **5**(4), 1379 (2005).

[53] G. H. Hwanga, W. K. Hana, S. J. Kima, S. J. Honga, J. S. Parkb, H. J. Parka, S. G. Kanga, Journal of Ceramic Processing Research, **10**(2), 190 (2009).

[54] X. Peng, L. Manna, W. Yang, J. Wickham, E. Scher, A. Kadavanich, A. P. Alivisatos, Nature, **404**(6773), 59 (2000).

[55] B. Li, M. Jing, G. Rong, Y. Xu, Y. Xie, European journal of inorganic chemistry, **2006**(21), 4349 (2006).

[56] D-F Zhang, L-D Sun, J. Zhang, Z-G Yan, C-H Yan, Crystal Growth and Design, **8**(10), 3609 (2008).

[57] B. Li, Y. Wang, The Journal of Physical Chemistry C, **114**(2), 890 (2009).

[58] J. Dharma, A. Pisal, C. Shelton, Simple method of measuring the band gap energy value of TiO2 in the powder form using a UV/Vis/NIR spectrometer, Application Note Shelton, CT: PerkinElmer, 2009.

[59] S. Zhang, R. Xiao, Journal of applied physics, **83**, 3842 (1998).

[60] S. P. Singh, B. Karmakar, Materials Chemistry and Physics, **119**(3), 355 (2010).

[61] J. I. Pankove, Optical processes in semiconductors, Courier Corporation, 2012.

[62] S. Qiang, C. Barthou, J. Denis, F. Pelle, B. Blanzat, Journal of Luminescence, **28**(1), 1 (1983).

[63] Z. Deng, F. Tang, A. J. Muscat, Nanotechnology, **19**(29), 295705 (2008).

_____

[*]Corresponding author: bhavaneeg@gmail.com